SANDIA REPORT

SAND2023-00634 Printed March 2023



On the constitutive stress-strain relationships and evaluation of the softening coefficient in work hardening mechanism

Alan F. Jankowski

Prepared by Sandia National Laboratories Albuquerque, New Mexico 87185 and Livermore, California 94550 Issued by Sandia National Laboratories, operated for the United States Department of Energy by National Technology & Engineering Solutions of Sandia, LLC.

NOTICE: This report was prepared as an account of work sponsored by an agency of the United States Government. Neither the United States Government, nor any agency thereof, nor any of their employees, nor any of their contractors, subcontractors, or their employees, make any warranty, express or implied, or assume any legal liability or responsibility for the accuracy, completeness, or usefulness of any information, apparatus, product, or process disclosed, or represent that its use would not infringe privately owned rights. Reference herein to any specific commercial product, process, or service by trade name, trademark, manufacturer, or otherwise, does not necessarily constitute or imply its endorsement, recommendation, or favoring by the United States Government, any agency thereof, or any of their contractors or subcontractors. The views and opinions expressed herein do not necessarily state or reflect those of the United States Government, any agency thereof, or any of their contractors.

Printed in the United States of America. This report has been reproduced directly from the best available copy.

Available to DOE and DOE contractors from U.S. Department of Energy Office of Scientific and Technical Information P.O. Box 62 Oak Ridge, TN 37831

> Telephone: (865) 576-8401 Facsimile: (865) 576-5728 E-Mail: reports@osti.gov

Online ordering: http://www.osti.gov/scitech

Available to the public from

U.S. Department of Commerce National Technical Information Service 5301 Shawnee Rd Alexandria, VA 22312

Telephone: (800) 553-6847 Facsimile: (703) 605-6900 E-Mail: orders@ntis.gov

Online order: https://classic.ntis.gov/help/order-methods/



ABSTRACT

The constitutive stress-strain relationships for structural alloys, such as additively manufactured Ti-6Al-4V, are reconstructed by assessing the form and mechanism of work hardening relationships. The stress-strain relationships are best fit using both the Hollomon and Voce expressions wherein the Voce expression well-reproduces the later stage(s) of work hardening whereas the Hollomon relationship provides a better fit just beyond the proportional limit.

Keywords: work hardening, softening coefficient, Voce, Hollomon, stress-strain modeling

ACKNOWLEDGEMENTS

The effort for this work was inspired by the objective to enhance the engineering application of structural AM materials. Any subjective views or opinions that might be expressed in the paper do not necessarily represent the views of the US Department of Energy or the United States Government. Sandia National Laboratories is a multi-mission laboratory managed and operated by National Technology & Engineering Solutions of Sandia, LLC, a wholly owned subsidiary of Honeywell International Inc, for the US Department of Energy's National Nuclear Security Administration under contract DE-NA0003525.

CONTENTS

Ab	ostract	3
Ac	knowledgements	4
Ex	ecutive Summary	7
Ac	ronyms and Terms	8
1.	Introduction	9
2.	Model	11
3.	Materials	15
4.	Results and Analysis	11
5.	Discussion and Conclusions	23
Re	ferences	25
Ap	pendix A	25
Ap	pendix B	25
Ap	pendix C	25
Di	stributionstribution	30
LIS	ST OF FIGURES	
	gure 1. The digitized true stress-strain curves for Ti-6Al-4V under tension [4] that represent a range of strength and ductility behavior. gure 2. The variation of work hardening with tensile stress [4] that corresponds with the stress-strain curves of Fig. 1.	
Fig	gure 3. The work hardening response for each Fig. 2 curve is modeled with linear (dashed) and curvilinear (dotted) stages that correspond to Voce and Hollomon stress-strain behavior, respectively.	
Fig	gure 4. The Fig. 3 stages of hardening are used to reconstruct examples of constitutive stress- strain curves (in this plot for samples 1-2, and 5-7) as governed by Voce (dashed) and Hollomon (dotted) behavior.	
Fig	gure 5. The softening coefficients c_b and c_{bi} of the integrated and stage responses of work	
	hardening, respectively, are plotted as a function of the plasticity ϵ as determined through the curve fits of Fig. 3 for the Voce and Hollomon stress-strain relationships	
LI	ST OF TABLES	
Та	blo 1. Work hardening parameters computed from true stress strain queries of Ti 6 AL AV	17

This page left blank

EXECUTIVE SUMMARY

Established engineering formulations allow engineers to quantify the scale of microstructure responsible for observed mechanical behavior. A dimensionless coefficient c_b was derived in accordance with the Kocks-Mecking work hardening behavior for a sample under tensile loading. The value for c_b is quantitatively determined by measuring the strength σ at the elastic limit, the strength at the instability point of localized deformation, and the amount of plastic strain ε between these strength limits. In practice, this c_b parameter allows one to track the changes in mechanical behavior that occurs with aging treatments, through different synthesis routes of the materials for comparative study, and for specifying the post-processing treatments needed to produce a prescribed mechanical response. This approach is useful in design specification as well as in qualification of material performance.

In this study, an analysis of the possible mechanisms of work hardening behavior are used to reconstruct constitutive equations that allow for the prediction of stress-strain behavior in Ti-6Al-4V, as well as determine which deformation mechanisms dominate the sequential stages of plastic deformation. It is seen that the Kocks-Mecking description of work hardening is derivative of the Voce expression for stress-strain behavior which predicts an asymptotic relationship for increased strength during deformation with plastic strain. In contrast, it's found that the Hollomon expression for stress-strain behavior provides an equally good fit to the early stages of work hardening, but a better fit to the stress-strain behavior beyond the initial yield point. This work is useful for clarifying the physical mechanisms that dominant deformation. Future work will permit more elaborate deformation routes to be analyzed including materials that undergo stress-induced phase transformations.

ACRONYMS AND TERMS

Acronym/Term	Definition
AM	additively manufactured
EBM	electron beam melting
SLM	selective laser melting
DMLS	direct metal laser sintering
fcc	face center cubic
hcp	hexagonal close packed
k _B	Boltzmann's constant
Т	temperature absolute
E	Elastic Young's Modulus
σ_{y}	proportional limit at initial yield
σ_{u}	ultimate strength at plastic instability
σ_{y}^{\star}	ratio of yield to ultimate strength
E	elastic Young's modulus
σ_{t}	true strength
$arepsilon_{t}$	true strain
ε_{p}	plastic strain
$arepsilon_{pi}$	plastic strain in stage "i"
C _b	softening coefficient for all stages
C _{bi}	softening coefficient in stage "i"
$\sigma_{\sf d}$	transition stress between stages 3 and 4
σ_{h}	Hollomon stress
σ_{v}	Voce stress
C _{pi}	Hollomon work-hardening constants
C _i	Voce stress constants
Θ_{i}	work hardening
Θ_3	working hardening in stage "i"
Θ_{oi}	work hardening coefficient intercept in stage "i"
Ė	strain rate
m	strain-rate sensitivity-of-strength exponent
ν*	activation volume
c _v *	activation volume coefficient

1. INTRODUCTION

There are two methods frequently used for describing the plasticity during deformation of a structural alloy. The general form of the Voce formulation [1] for stress σ takes form with an Arrhenius relationship with a negative exponential function of strain e as shown in eqn. (1), wherein ε_0 is the strain at the proportional limit. The general form of the Hollomon equation [2] that provides a power law representation of stress increasing as a function of strain to an exponent n is shown in eqn. (2). The exponent n is bounded by zero (for a perfectly plastic solid) and one (for a perfectly elastic solid). For many metals, the exponent n for eqn. (2) is typically between 0.1 and 0.5. In these relationships, the c-values are constants.

$$\sigma_{v} = c_{1} \cdot \left[1 - c_{2} \cdot e^{-c_{3} \cdot (\varepsilon - \varepsilon_{0})}\right] \tag{1}$$

$$\sigma_{b} = c \cdot (\varepsilon - \varepsilon_{o})^{n} \tag{2}$$

The Hollomon expression [2] often works well at the outset of plastic deformation, but overestimates strengthening as it produces an ever-increasing strength with the progression of plastic strain towards failure. The rapid increase in stress with plastic deformation can be related to the activation and continuous generation of dislocations. However, in practice, there is a limit and leveling to the increase in stress from work hardening as can be described by the Voce formulation [1] of strength. Progression of deformation occurs through the generation and annihilation of dislocations in a steady-state manner. The negative-exponential to a power of the strain in eqn. (1) produces the Arrhenius-type statistical leveling of the stress to the pre-factor coefficient. To further investigate the application in each approach, an examination is now pursued to the variation in the instantaneous slope $(\partial \sigma/\partial \epsilon)$ of the stress-strain curve with increasing stress σ . The work hardening Θ is described by the following formulation.

$$\Theta = \partial \sigma / \partial \varepsilon \tag{3}$$

The variation in work hardening Θ as a function of stress s is seen in Kocks-Mecking plots [3] that can provide insight to the stages of plastic deformation where the Hollomon or Voce relationships are evident. The plasticity stages align with a decrease in Θ as σ increases, following a region where the slope of the stress-strain curve is constant, that where Θ equals the elastic modulus E. The curvilinear relationships within the work hardening plot of σ versus Θ can be formulated by substitution of: eqn. (1) into the partial differential of eqn. (3) for evidencing Voce behavior; and

eqn. (2) into (3) for evidencing Hollomon behavior. An assessment is now made to compare the contributions of each stress-strain behavior in the work hardening assessment of additively manufactured Ti-6Al-4V alloys. Samples are selected for analysis that offer a range in strength and ductility.

2. MODEL

2.1. Voce Behavior

For the assessment of the Voce relationship of stress σ_v with plastic strain ε , the substitution and reduction of the Voce-based formulation input into the partial differential for work hardening Θ is now considered. In the following steps of the derivation, note that eqn. (1) is rewritten in terms of $(c_1 - \sigma)$ when substituted into eqn. (4e). Equation (1) is inserted into eqn. (4a) to arrive at eqn. (4b). Terms are separated in eqn. (4c), where the partial derivative of the constant is equated to zero in eqn. (4d). The partial derivative of eqn. (4d) is solved in eqn. (4e), and eqn. (1) is again introduced into this solution to arrive at eqn. (4f). Terms are separated in eqn. (4g) to produce the recognizable form of a linear equation for work hardening Θ .

$$\Theta = \partial \sigma_{i} / \partial \varepsilon \tag{4a}$$

$$\Theta = \partial [c_1 \cdot (1 - c_2 \cdot e^{-c_3 \cdot \varepsilon})] / \partial \varepsilon$$
 (4b)

$$\Theta = \partial(c_1)/\partial \varepsilon - \partial(c_1 \cdot c_2 \cdot e^{-c_3 \cdot \varepsilon})/\partial \varepsilon$$
(4c)

$$\Theta = 0 - \mathbf{c}_{1} \cdot \mathbf{c}_{2} \cdot \partial (\mathbf{e}^{-\mathbf{c}_{3} \cdot \mathbf{\epsilon}}) / \partial \mathbf{\epsilon}$$
(4d)

$$\Theta = (-\mathbf{c}_1 \cdot \mathbf{c}_2) \cdot (-\mathbf{c}_3) \cdot \mathbf{e}^{-\mathbf{c}_3 \cdot \mathbf{\epsilon}} = \mathbf{c}_3 \cdot (\mathbf{c}_1 \cdot \mathbf{c}_2 \cdot \mathbf{e}^{-\mathbf{c}_3 \cdot \mathbf{\epsilon}})$$

$$\tag{4e}$$

$$\Theta = c_3 \cdot (c_1 - \sigma_v) \tag{4f}$$

$$\Theta = c_3 \cdot c_1 - c_3 \cdot \sigma_v \tag{4g}$$

The general form of eqn. (4g) is shown in eqn. (5). This is the Kocks-Mecking form that utilizes a linear relationship of the work hardening Θ as a function of stress σ .

$$\Theta = \Theta_{0} - c_{b} \cdot \sigma \tag{5}$$

The coefficients c_1 and c_3 are uniquely determined by fitting the corresponding Kocks-Mecking (K-M) work hardening stage of Voce behavior. A solution for the coefficient c_2 is readily available using eqn. (1) once the curvilinear fit of eqn. (5) is known for the variation of Θ with σ . The plasticity of a material during work hardening that follows a Voce relationship for stress-strain

behavior of eqn. (1) is seen as a linear curve in a Kocks-Mecking plot of work hardening versus stress following the relationship of eqn. (5). The coefficients of the Voce expression in eqn. (1) for

the constitutive relationship between stress and strain can be uniquely determined using the linear fit of eqn. (5) in a Kocks-Mecking plot as constructed directly from experimental data. If a transition occurs from the governing constitutive Voce relationship into another as seen in the change in slope of the linear curve, then multiple linear regions will be present in the Kocks-Mecking plot, each with its own unique set of coefficients Θ_{ci} and c_{bi} .

A formulation for the decrease in the work hardening Θ with applied stress σ for structural metals as stainless steel and titanium alloys has been approached [4] using two sequential linear regions of Kocks-Mecking stages 3 and 4, with slopes c_{b3} and c_{b4} , respectively. In these stages, the work hardening mechanism is first initiated with the activation of dislocations, then progressives by the generation and annihilation of dislocations. The Kocks-Mecking relationship of eqns. (4g)-(5) takes the general form in eqn. (6) for each stage of K-M work hardening where Θ_{oi} is intercept value of work hardening Θ_i at zero stress.

$$\Theta_{i} = \Theta_{oi} - c_{bi} \cdot \sigma_{i} \tag{6}$$

This approach to separate sequential stages is used for two purposes. One purpose [4] is the derivation of an expression that relates the strain rate sensitivity of strength exponent m and the activation volume for deformation v^* with the softening coefficient c_{b3} as shown in eqn. (7). Details of this derivation are in Appendix A.

$$\upsilon^* = (c_{b3}/m) \cdot [(k_B \cdot T)/(\Theta_{o3} - E)] \tag{7}$$

This occurs in stage 3 as the deformation first proceeds from the elastic to plastic region. Here, the activation volumetric coefficient c_{u^*} is shown [4] to equal $(k_B \cdot T)/(\Theta_{o3} - E)$ where k_B is Boltzmann's constant, T is temperature absolute, and E is the elastic modulus. From eqn. (7), the activation volume for deformation can be determination from a single stress-strain curve providing an approximation of the strain rate sensitivity of strength is provided. Alternatively, the strain rate sensitivity can be approached from a single stress-strain curve using a value provided for the activation volume.

The second purpose [4] for a multiple-stage analysis is used to distinguish individual components c_{b3} and c_{b4} with the softening coefficient c_b for stages 3 and 4, respectively. Here, the distinction of c_{bi} in stages 3 and 4 is made in comparison to an integral value of c_b for the entire plastic region as first presented by Morris, Jr. [5] in eqn. (8) and developed [4][6][7] in application to trace the changes in

mechanical behavior with post-processing thermal-aging treatments of additively manufactured (AM) alloys. Details of this derivation are in Appendix B.

$$\varepsilon_{p} = (c_{b})^{-1} \cdot \ln \left[1 + c_{b} \cdot (1 - \sigma_{v} \cdot \sigma_{u}^{-1}) \right]$$
 (8)

The singular value of c_b was formulated assuming a constant linear variation for decreasing Θ with increasing applied stress σ for the entire range of: plastic strain ε_p (from the strain ε_p at yield to the strain ε_p at the instability); and stress σ (from the proportional limit σ_p to the instability point) where the useable ultimate strength σ_p is determined from the subtangent Considère construct of true stress σ versus strain ε . In practice, the intercept point of σ_p between stages 3 and 4 can be evaluated and used to determine c_p of eqn. (1) for each curvilinear Voce portion in the Θ versus σ_p plot as detailed in Appendix C.

2.2. Hollomon Behavior

Just as the linear form in a Kocks-Mecking plot can be determined from the negative exponential form of the Voce expression for stress versus strain, it's possible to assess and provide constitutive equations for stress-strain behavior that are derived from (and approximate) the sequential stages of work hardening for structural alloys. In addition to the linear response of work hardening with stress, a power law relationship can be assumed for the work hardening variation with stress up to the instability. A power law relationship using a negative exponent produces the behavior for a rapid decrease in Θ followed by a leveling in the decrease as s continues to increase in from stage 3 into 4. This behavior is described by eqn. (9) in considering the variation of Θ with σ

$$\Theta = c_{p1} \cdot \sigma^{-c_{p2}} \tag{9}$$

In eqn. (9), c_{p_1} and c_{p_2} are constants. The tangent to this curve at the beginning of plastic deformation, i.e. the proportional limit, has an equivalent slope that corresponds to negative c_{b3} . Similarly, the tangent at the instability has an equivalent slope that corresponds to negative c_{b4} . The governing relationship between stress and strain (to the instability) that is shown in eqn. (10) is determined by equating eqns. (3) and (9). A derivation using partial integration follows as eqn. (10) is multiplied by $\sigma^{c_{p2}}$ and integrated over $\partial \varepsilon$ to arrive at eqn. (11) and solved in eqn. (12). The expression for stress s in eqn. (13) is next determined by placing the terms of eqn. (12) to the power n of $[1/(c_{p_2}+1)]$.

$$\partial \sigma / \partial \varepsilon = c_{p_1} \cdot \sigma^{c_{p_2}} \tag{10}$$

$$\int \sigma^{c_{p2}} \cdot \partial \sigma = \int c_{p_1} \cdot \partial \varepsilon \tag{11}$$

$$\sigma^{c_{p_2}+1} = c_{p_1} \cdot (c_{p_2}+1) \cdot \varepsilon \tag{12}$$

$$\sigma = \left[c_{p_1} \cdot (c_{p_2} + 1) \cdot \varepsilon\right]^{[1/(c_{p_2} + 1)]} \tag{13}$$

Equation (13) is then reduced, producing the Hollomon expression in eqn. (2) where the constant c equals $[c_{p_1}\cdot(c_{p_2}+1)]^n$. Here, it's shown that a decaying curvilinear response in the work hardening curve that appears beyond the proportional limit can be reproduced using the Hollomon form of the stress-strain relationship.

3. MATERIALS

The new approach for independently assessing the work hardening stages and underlying Voce and Hollomon mechanisms is evaluated for eight Ti-6Al-4V samples, as tested under quasi-static uniaxial tension at strain rates less than 2·10⁻⁴ s⁻¹. These tensile samples are selected from a broader study [4] [7][8] of Ti-6Al-4V produced by different AM process methods [9][10][11][12][13]. These AM methods include electron beam melting (EBM), selective laser melting (SLM), and direct metal laser sintering (DMLS). The microstructures of these Ti-6Al-4V samples include variants of martensite, alath and a+b phases in the as-deposited condition as well as after thermal-mechanical aging. These nominally (>97%) dense AM samples provide a representative sampling of synthesis and processing methods with a concurrent wide range of tensile behaviors.

The Ti-6Al-4V samples selected from the c_b-analysis of tensile tests [7] are evaluated within the distinct work hardening stages using the above formulations. Eight representative stress-strain curve results [8][9][10][11][12][13] were digitized and replotted from Jankowski [4] as the variation in true stress s as a function of true strain e as shown in Figure 1.

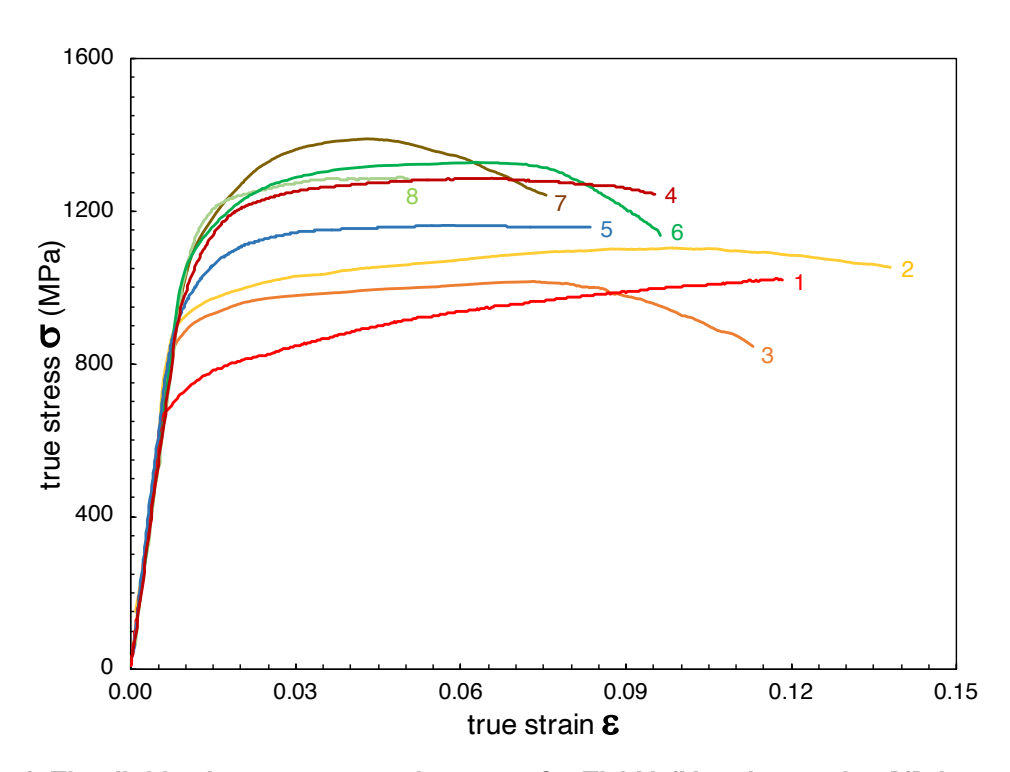


Figure 1. The digitized true stress-strain curves for Ti-6Al-4V under tension [4] that represent a range of strength and ductility behavior.

An intrinsic error occurs in the accuracy of the digital scan of each stress-curve curve. The measurement errors are $\Delta\sigma$ of ± 2 MPa, $\Delta\epsilon$ of ± 0.0002 , and ΔE ± 1 GPa. The elastic loading regime for these results is consistent with the nominal value of a 114 GPa elastic modulus. A three-point computation of slope is used to calculate the work hardening Θ from the stress-strain curve of Figure 1. A five-point weighted average is then used to smooth the instantaneous value for slope. The work hardening Θ versus true stress σ_t plots are shown in Figure 2, correspondingly, as replotted from Jankowski [4].

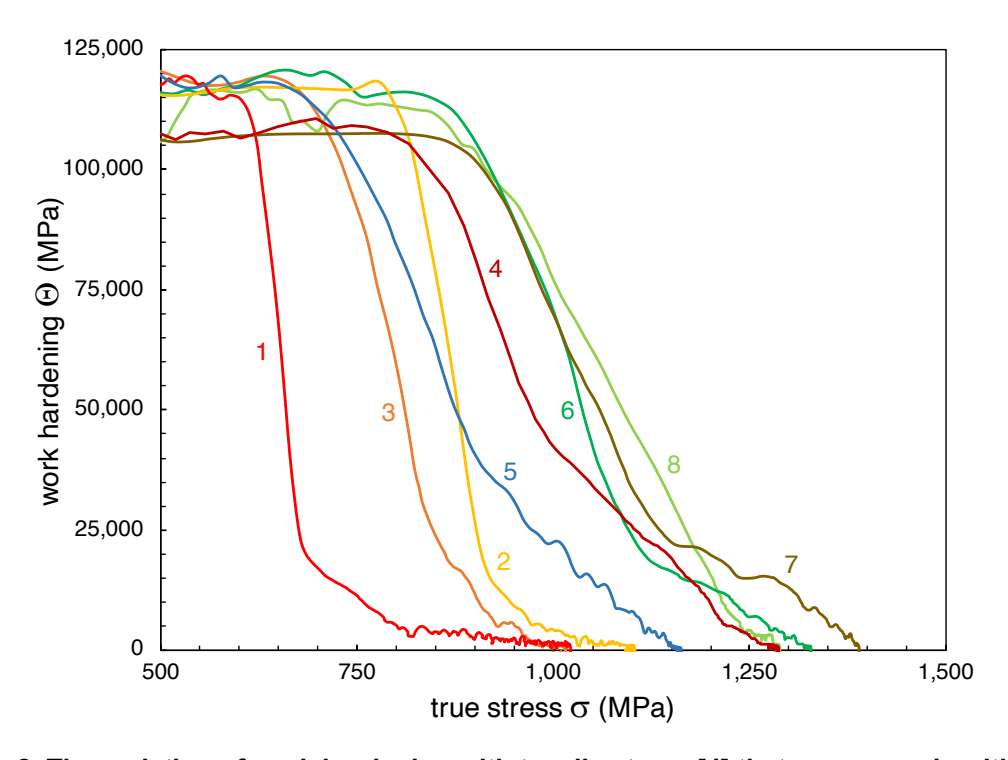


Figure 2. The variation of work hardening with tensile stress [4] that corresponds with the stress-strain curves of Figure 1.

The softening factor c_b for each sample was computed using eqn. (8) with the measured plastic strain ϵ_p between the proportional limit σ_y and the stress σ_u at plastic instability. The elastic regime is determined by a linear fit of initial loading in the Fig. 2 stress-strain curves. The point at which stress deviates from linearity, as fit to a correlation coefficient of $R^2 \ge 0.98$, is used to identify the σ_y -value for the proportional limit. The subtangent construct was used to determine the instability stress σ_u from the Considère criterion using curves of the true stress versus engineering strain. The σ_y , σ_u , ε_p , and E values for the eight Ti-6Al-4V samples are list in Table 1 as reproduced from Jankowski [4].

Table 1. Work hardening parameters computed from true stress-strain curves of Ti-6Al-4V								
sample no.	1	2	3	4	5	6	7	8
σ _u (MPa)	1022	1098	1015	1283	1162	1319	1389	1284
$\sigma_{_{\!\scriptscriptstyle V}}^{*}$	0.63	0.74	0.75	0.72	0.68	0.73	0.68	0.73
ϵ_{p}	0.112	0.076	0.065	0.047	0.046	0.037	0.035	0.029
c_{b}	18.3±0.1	27.2±0.2	34.7±0.3	62.0±0.5	67.2±0.5	85.9±0.9	100±1.0	123±1.5
ϵ_{p3}	0.0017	0.0028	0.0031	0.0024	0.0027	0.0029	0.0038	0.0085
ϵ_{p4}	0.110	0.067	0.055	0.040	0.035	0.032	0.030	0.018
c ₁ (MPa)	693.0	928.6	875.8	1080.6	988.2	1153.8	1194.2	1248.9
c_2	0.006145	0.007854	0.012225	0.050467	0.060692	0.044586	0.054640	0.017286
c ₃ , c _{b3V}	1505±9	975±2	759±8	450±3	450±3	438±4	362±1	313±2
$c_{ m b4V}$	16.6±2.9	28.1±9.3	38.0±15.2	74.5±3.4	89.4±19.6	87.5±6.4	96.0±3.4	93.9±15.9
σ _d (MPa)	689	921	865	1026	928	1102	1129	1227
Θ _{o3} (GPa)	1043±6	905±2	665±7	487±3	445±2	506±5	432±2	391±2
Θ _{o4} (GPa)	17.8±3.1	33±11	41±16	101±5	110±24	119±9	132±5	122±21
E (GPa)	118	121	120	107	122	115	107	109
$c_{v^*} (10^{-6} \text{ nm}^3)$	4.38	5.16	7.43	10.7	12.5	10.3	12.5	14.4
υ* (nm³)	0.470	0.359	0.403	0.343	0.403	0.324	0.322	0.321
c _{p1}	1.8296 • 1033	1.3158·1053	8.4879.1038	4.7282.1025	3.6586·10 ²⁶	4.9769 • 1029	5.9103.1023	1.3316·1019
c _{p2}	10.163	16.514	11.832	7.0147	7.4296	8.3157	6.3229	4.7455
c _{b3H}	1506	1326	1052	594.8	1042	620.7	432.3	516.8
c _{b4H}	10.7	19.1	26.6	40.7	39.4	35.4	54.1	87.3
c (MPa)	1184.86	1270.68	1318.92	2071.20	1824.02	1958.24	2313.58	2889.09
n	0.089585	0.057099	0.077933	0.124770	0.118630	0.107345	0.136558	0.174050
material	wire	z- EBM	x- SLM+HIP	x- SLM	z- DMLS	x- SLM	z- SLM	x- SLM
reference	8	13	14	13	11	12	14	15

Notations for the tensile test conditions are x-axis for longitudinal and y-axis for transverse directions within the build plane, along with z-axis for the vertical direction from the build plate. The data of Table 1 is arranged in order of increasing c_b value, and decreasing plastic strain ϵ_p .

4. RESULTS AND ANALYSIS

4.1 Reconstructing Constitutive Stress-Strain Relationships

An analysis of the work hardening curves plotted in Figure 2 was made [4] to assess an activation volume for the onset of plasticity for the Ti-6-4 alloys previously reported [7]. Further analysis is now pursued to assess the different mechanisms of Voce and Hollomon stress-strain behavior as well as the effects of work hardening seen in the Figure 3 plots. Linear fits (shown with dashed lines) in Figure 3 are provided in accordance with eqn. (6) for both stages 3 and 4 of work hardening, corresponding with the Voce relationship of eqn. (1). The values of c_1 , c_2 , and c_3 are computed using the procedure detailed in Appendix C. These c_1 , c_2 , and c_3 values along with the corresponding c_{bi} of stages 3 and 4 for the Voce relationship are listed on Table 1.

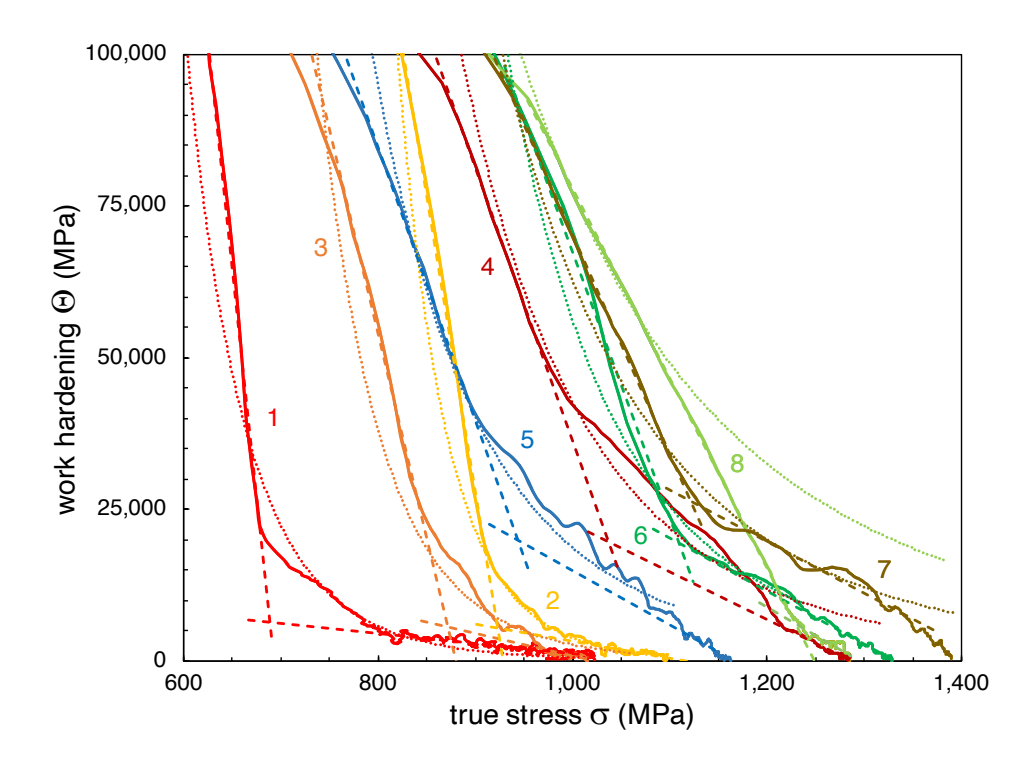


Figure 3. The work hardening response for each Figure 2 curve is modeled with linear (dashed) and curvilinear (dotted) stages that correspond to Voce and Hollomon stress-strain behavior, respectively.

The eqn. (9) construct for the Hollomon relationship, as seen with the curvilinear fit (shown with dashed lines), is now made to best fit the onset of plastic deformation at the proportional limit. The coefficients c_{p_1} and c_{p_2} fit to eqn. (9) are listed in Table 1 along with the corresponding values computed using eqn. (13) for the coefficients c and n in the Hollomon relationship of eqn. (2). The

Hollomon expression doesn't contain a parameter equivalent to the softening coefficient as expressed in the Kocks-Mecking relationship of eqn. (5) as derived from the Voce relationship, or in the distinct work hardening stages of eqn. (6). However, an equivalence with c_{b3} and c_{b4} can be approximated by considering the slope of the curvilinear response in Figure 3 at the onset of deformation and at the instability, respectively. That is, from the Hollomon analysis, the absolute value of the slope at the proportional limit σ_y and instability σ_u is approximates the c_{bi} -value from the Voce analysis for stages 3 and 4, with corresponding values of c_{b3} and c_{b4} . These c_{bi} -values can be computed using the following eqn. (14), that equals the differential of eqn. (9) with respect to stress σ as

$$c_{bi} = |\partial\Theta/\partial\sigma| = c_{p1} \cdot c_{p2} \cdot \sigma^{(-c_{p2}-1)}$$
(14)

Values for c_{p_1} and c_{p_2} are listed in Table 1, with corresponding c_{bi} values for stages 3 and 4 as computed at the proportional and instability, respectively. An additional subscript of H or V (for c_{bi}) are used to differentiate these values computed in accordance with the Voce and Hollomon expressions, respectively.

The constitutive parameters of both the Voce and Hollomon expressions in eqns. (1-2) are listed in Table 1 and can now be used to plot simulated stress-strain behavior as determined through the analysis of the work hardening curves in Figure 3. The simulated stress-strain results are plotted in Figure 4 wherein the Voce relationship for stages 3 and 4 are plotted (dashed curves) along with the (dotted curve) result for the Hollomon relationship. As attributed to the asymptotic nature of the Voce expression, this relationship does not well simulate the actual behavior in stage 3, although the initial slope c_{b3V} in stage 3 is well fit. A better fit to the stress-strain data is found through the Hollomon expression that works well beyond the proportional limit for all curves in stage 3. Values similar to c_{bi3} are found for c_{bi3} using the Hollomon expressions as listed in Table 1. However, as the amount of strengthening increases during work hardening (and the accompanying amount of plasticity decreases), the Voce model provides a better fit to simulate the stress-strain behavior to the instability whereas the Hollomon curve overestimates strengthening. The calculation of an activation volume v* that corresponds to the onset of deformation represents the volume of dislocations mobilized is accomplished using eqn. (7). Values of v* are reproduced from the K-M analysis using the Voce formulation [4] as listed in Table 1.

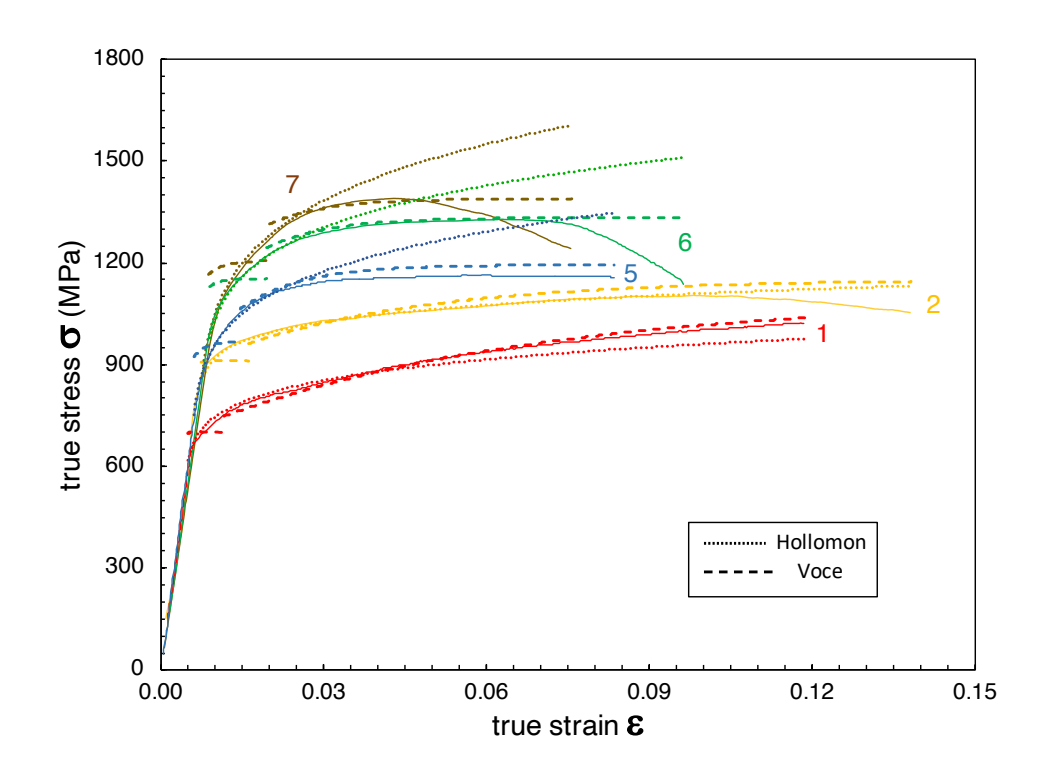


Figure 4. The Figure 3 stages of hardening are used to reconstruct examples of constitutive stress-strain curves (in this plot for samples 1-2, and 5-7) as governed by Voce (dashed) and Hollomon (dotted) behavior.

The υ^* -value decreases from 0.47 to 0.32 nm³ as the amount of plastic strain decreases from 0.11 to 0.03. The c_{b3H} -estimate from the Hollomon analysis produces a result similar in value to the Voce c_{b3V} results, where a decrease from 1.51·10³ to values less than 0.5·10³ occurs as the plastic strain ε_p between the proportional limit and instability decreases from 0.11 to 0.03.

4.2 Softening Coefficients c_{bi} of Work Hardening Stages

The variation in the measured plastic strain ε_p with the computed softening factor c_{bi} is plotted in Figure 5. Values are plotted for: the integrated model that assumes one hardening stage (c_b) according to eqn. (5); stages 3 and 4 of work hardening (c_{biV}) in accordance with eqn. (6) and the Voce stress-strain relationship; and stages 3 and 4 (c_{biH}) as determined with eqn. (14) for Hollomon stress-strain behavior. The distribution of c_b values illustrate the range of plastic strain ε_p associated with the different processing conditions selected for this sample set. As noted in Sec. 4.1, the fitted c_{b3V} and modeled c_{b3H} values decrease with the total plastic strain and are high for the narrow range of strain associated with stage 3 accompanied by a large drop in stress. The stage 4 c_b -values are

similar to the integrated value and increase from 10-to-100 with a progressive decrease in the total plastic strain.

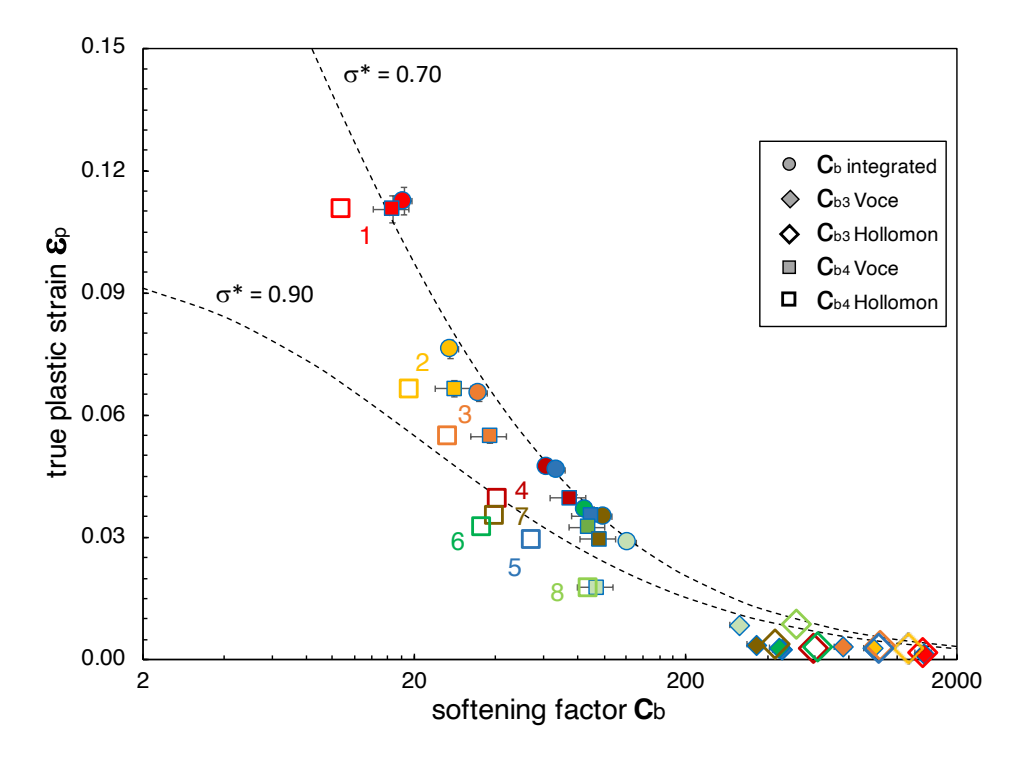


Figure 5. The softening coefficients c_b and c_{bi} of the integrated and stage responses of work hardening, respectively, are plotted as a function of the plasticity ϵ as determined through the curve fits of Figure 3 for the Voce and Hollomon stress-strain relationships.

The measurement errors from the digitization process of the stress-strain curves are shown as input to the computation of c_b to determine the Δc_b value. An average σ_y^* value of 0.72 ± 0.03 is computed for the AM samples for work hardening in accordance with the linear variation associated with the Voce relationship. The σ_y^* value for the integrated c_b -computation is larger than 0.63 value for the Ti-6Al-4V wire sample. The higher σ^* -value for AM product versus the wrought form is seen as well for the analysis of 316L tensile test results [6]. The dashed curves in Fig. 5 represents idealized results for the c_b variation with ϵ_p using eqn. (8) where σ^* are set equal to 0.70 and 0.90. In general, the stage 4 c_b -values are slightly larger than the integrated values but rest within the computed Δc_b -error bars.

5. DISCUSSION AND CONCLUSIONS

The work hardening behavior of AM Ti-6Al-4V has been assessed using a linear variation with stress in accordance with the Kocks-Mecking analysis as based on Voce stress-strain behavior. In addition, a curvilinear relationship of work hardening using a negative exponent of stress is assessed, as derivative from Hollomon stress-strain behavior. Both approaches produce similar values for softening coefficients that are associated with the linear K-M work hardening stages. With the use of the work hardening relationships to identify the dominate range of operative stress-strain mechanisms, in this case a comparison of Voce and Hollomon, it is found that the Hollomon relationship better simulates the early stage of work hardening beyond the proportional limit, whereas the Voce relationship best simulates the later stages of deformation to the instability. These results are consistent with structural alloys that undergo work hardening as a distinct increase in dislocation density beyond the proportional limit is followed by a saturation in dislocation and a leveling in the strengthening to the instability.

This page left blank

REFERENCES

- [1] Voce E. The Relationship Between Stress and Strain for Homogeneous Deformation. J. of the Institute Metals 1948; 74: 537–562.
- [2] Hollomon JR. Tensile deformation. Trans. of AIME 1945; 162: 268–277.
- [3] Kocks UF, Mecking H. Physics and phenomenology of strain hardening: the FCC case. Prog Mater Sci. 2003; 48: 171-273. doi:10.1016/S0079-6425(02)00003-8.
- [4] Jankowski AF. A model for the softening factor within stages of work hardening. (SAND2023-00635).
- [5] Morris, Jr. JW. Is there a future for nanostructured steel? in 16th International Society for Offshore and Polar Engineering Conf Proc., ISOPE 2007: 2814–2818.
- [6] Jankowski AF, Yang N, Lu W-Y. Constitutive structural parameter c_b for the work hardening behavior of laser powder-bed fusion, additively manufactured 316L stainless steel. Mater Des Proc Comm. 2020; 2: e96-1-9. doi:10.1002/mdp2.135.
- [7] Jankowski AF. A constitutive structural parameter c_b for the work hardening behavior of additively manufactured Ti-6Al-4V. Material Design and Processing Communication 2021; e262-1-9. doi:10.1002/mdp2.262.
- [8] Jankowski AF, Chames JM, Gardea A, Nishimoto R, Brannigan EM The softening factor c_b of commercial titanium alloy wires. Intern J Mater Res. 2019; 110: 990-999. doi:10.3139/146.111834.
- [9] Fadida R, Shirizly A, Rittel D. Dynamic Tensile Response of Additively Manufactured Ti-6Al-4V with Embedded Spherical Pores. J. Appl. Mech. 2018; 85: 041004-1-10. doi:10.1115/1.4039048.
- [10] He B, Wu W, Zhang L, Lu L, Yang Q, Long Q, Chang K. Microstructural characteristic and mechanical property of Ti-6Al-4V alloy fabricated by selective laser melting. Vacuum 2018; 150: 79-83. doi:10.1016/j.vacuum.2018.01.026.
- [11] Leicht A, Wennberg E. Analyzing the Mechanical Behavior of Additive Manufactured Ti-6Al-4V Using Digital Image Correlation. Diploma work no. 157, SP Techn. Res. Instit. Sweden, Chalmers Univ. Technol. 2015; Gothenburg: 51 pages.
- [12] Tao P, Li H-X, Huang B-Y, Hu Q-D, Gong S-L, Xu Q-Y. Tensile behavior of Ti-6Al-4V alloy fabricated by selective laser melting: effects of microstructures and as-built surface quality. Res. Dev. China Foundry 2018; 15(4): 243-252. doi:10.1007/s41230-018-8064-8.
- [13] Voisin T, Calta NP, Khairallah SA, Forien J-B, Balogh L, Cunningham RW, Rollett AD, Wang YM. Defects-dictated tensile properties of selective laser melted Ti-6Al-4V. Mater Des. 2018; 158: 113-126. doi:10.1016/j.matdes.2018.08.004.
- [14] Gibbs GB. Thermodynamic Analysis of Dislocation Glide Controlled by Dispersed Local Obstacles. Mater Sci Eng. 1969; 4:313–328.
- [15] Cahn JW, Nabarro FRN. Thermal Activation Under Shear. Phil Mag. 2001; 81:1409–1426. doi:10.1080/01418610108214448.

APPENDIX A

The initiation of plasticity in Stage 3 corresponds with activating a volume υ^* of dislocations under shear as formulated [14-15] in eqn. (A.1). The variables are absolute temperature T (K) and strain rate $\dot{\varepsilon}$ (s⁻¹), and k_B is the Boltzmann constant 1.38065·10⁻²³ J·K⁻¹. The Dorn equation for the strain-rate sensitivity of strength is shown in eqn. (A.2) from which the strain-rate sensitivity exponent (m) can be derived and then related to the softening coefficients and activation volume, as follows.

$$\upsilon^* = k_B \cdot T \cdot [\partial(\ln \dot{\varepsilon})/\partial(\sigma)] \qquad (A.1)$$

$$\sigma = c \cdot (\dot{\varepsilon})^m \qquad (A.2)$$

$$m \cdot (\ln \dot{\varepsilon}) = \ln(\sigma) - \ln(c) \qquad (A.3) \text{ take natural log of (A.2) and solve for m}$$

$$\partial(\ln \dot{\varepsilon})/\partial(\sigma) = (m \cdot \sigma)^{-1} \qquad (A.4) \text{ partial differential of (A.3) with respect to } \sigma$$

$$\upsilon^* = k_B \cdot T \cdot (m \cdot \sigma)^{-1} \qquad (A.5) \text{ substitute (A.4) into (A.1) and solve for } \upsilon^*$$

$$\Theta_i = \Theta_{oi} - [(k_B \cdot T) \cdot c_{bi} \cdot (m \cdot \upsilon^*)^{-1}] \qquad (A.6) \text{ substitute (A.5) into eqn. (6)}$$

An expression for v^* can now be deduced, as a function of c_{b3} using (A.6), to reveal the following relationship between the activation volume and the underlying scale of microstructure that accompanies the onset of work hardening in Stage 3.

$$\begin{split} \Theta_3 &= \Theta_{o3} - [(k_B \cdot T) \cdot c_{b3} \cdot (m \cdot \upsilon^*)^{-1}] & (A.7) \text{ substitute i equals 3 with stage 3} \\ \upsilon^* &= (c_{b3}/m) \cdot [(k_B \cdot T)/(\Theta_{o3} - \Theta_3)] & (A.8) \text{ solve (A.7) for } \upsilon^* \\ \upsilon^* &= (c_{b3}/m) \cdot [(k_B \cdot T)/(\Theta_{o3} - E)] & (A.9) \text{ rewrite (A.8) noting that } \Theta_3 = \Theta_2 = E \text{ at the yield point to arrive at eqn. (7)} \\ \upsilon^* &= c_{\upsilon^*} \cdot (c_{b3}/m) & (A.10) \text{ rewrite (A.9) noting } c_{\upsilon^*} \text{ equals } [(k_B \cdot T)/(\Theta_{o3} - E)] \end{split}$$

Equation (A.10) provides proof that the softening coefficient c_b well represents the activation volume v^* for deformation. The proportional relationship between v^* and (c_{b3}/m) indicates that a smaller activation volume will be commensurate with materials that have a high exponent m for its strain-rate sensitivity of strength.

APPENDIX B

The amount of work hardening (Θ) that remains decreases linearly with the progression of increased load, i.e. stress (σ) , in a manner proportion to the scale of microstructure. This Kocks-Mecking relationship is a direct derivation from the Voce expression for the variation of stress with strain as detailed above. J.W. Morris, Jr. developed [5] an expression for determination of the scale of the refined microstructures (as represented by decreasing c_b values) that extend the range of plasticity (ε) . A detailed derivation for determining the softening coefficient c_b dependence on the ratio of the yield to ultimate strengths and the amount of plastic strain between these limits is provided as follows.

- $\Theta = \partial \sigma / \partial \epsilon$
- $\Theta^{-1} = \partial \epsilon / \partial \sigma$
- $\Theta = \Theta_{o} c_{b} \cdot \sigma$
- $-c_{l_{s}} = \partial \Theta / \partial \sigma$
- $-c_b^{-1} = \partial \sigma / \partial \Theta$
- $\varepsilon = \int \partial \varepsilon = \int (\partial \varepsilon / \partial \sigma) \, \partial \sigma$
- $\varepsilon = \int (\Theta^{-1}) \partial \sigma$
- $\varepsilon = \int (\partial \sigma/\Theta) \cdot (\partial \Theta/\partial \sigma) \cdot (\partial \sigma/\partial \Theta)$
- $\epsilon = \int (\partial \Theta/\Theta) \cdot (\partial \sigma/\partial \Theta)$
- $\varepsilon = -c_b^{-1} \cdot \int (\partial \Theta/\Theta)$
- $\epsilon_{p} \equiv -c_{b}^{-1} \cdot [\ln \Theta_{u} \ln \Theta_{y}]$
- $\epsilon_{p} \equiv c_{b}^{-1} \cdot [\ln \Theta_{y} \ln \Theta_{u}]$
- $\Theta_{\rm u} = \sigma_{\rm u}$
- $\varepsilon_{\rm p} = c_{\rm b}^{-1} \cdot [\ln \Theta_{\rm v} \ln \sigma_{\rm u}]$
- $\varepsilon_{p} = c_{b}^{-1} \cdot \ln(\Theta_{y}/\sigma_{u})$
- $\Theta_{y} \equiv \Theta_{o} c_{b} \cdot \sigma_{y}$
- $\Theta_{\rm u} \equiv \Theta_{\rm o}$ $c_{\rm b}$ · $\sigma_{\rm u}$
- $\boldsymbol{\Theta}_{_{\boldsymbol{o}}} = \boldsymbol{\Theta}_{_{\boldsymbol{u}}} + \boldsymbol{c}_{_{\boldsymbol{b}}} \boldsymbol{\cdot} \boldsymbol{\sigma}_{_{\boldsymbol{u}}}$
- $\Theta_{o} = \sigma_{u} + c_{b} \cdot \sigma_{u}$

- (B.1a) slope of stress strain
- (B.1b) slope of stress strain
- (B.2) K-M relationship
- (B.3) slope of (B.2)
- (B.4) invert (B.3)
- (B.5) definition of strain
- (B.6) substitute (B.1b) into (B.5)
- (B.7) unity $(\partial \Theta/\partial \sigma) \cdot (\partial \sigma/\partial \Theta)$ times (B.6)
- (B.8) re-group (B.7) terms
- (B.9) substitute (B.4) into (B.8)
- (B.10) evaluate integral of (B.9) from yield to instability
- (B.11) re-write (B.10)
- (B.12) defining condition at the instability (stage V onset)
- (B.13) substitute σ_u equals Θ_u into (B.11)
- (B.14) re-write ln-expression of (B.13)
- (B.15a) substitute $\sigma = \sigma_v$ into (B.2) at yield
- (B.15b) substitute $\sigma = \sigma_{u}$ into (B.2) at the instability
- (B.15c) substitute $\sigma = \sigma_u$ into (B.2) at the instability
- (B.15d) substitute (B.12) into (B.15c) at the instability

$$\Theta_{o} = \sigma_{u} \cdot (1 + c_{b})$$

(B.15e) group terms in (B.15d)

$$\varepsilon_{p} = c_{b}^{-1} \cdot \ln \left[(\Theta_{o} - c_{b} \cdot \sigma_{y}) / \sigma_{u} \right]$$

(B.16) substitute (B.15a) into (B.14)

$$\epsilon_{p} \equiv c_{b}^{-1} \cdot ln \ \{ [\sigma_{u} \cdot (1 + c_{b}) - c_{b} \cdot \sigma_{y}] / \sigma_{u} \} \ (B.17) \ substitute \ (B.15e) \ into \ (B.16)$$

$$\varepsilon_p = c_b^{-1} \cdot \ln \left[(1 + c_b) - (c_b \cdot \sigma_y / \sigma_u) \right]$$

(B.18) separate terms with In-term by divisor in (B.17)

$$\varepsilon_p = c_b^{-1} \cdot \ln \left[(1 + c_b) - (c_b \cdot \sigma^*) \right]$$

(B.19) substitute σ^* equals (σ_y/σ_u) into (B.18)

$$\varepsilon_{p} = c_{b}^{-1} \cdot \ln \left[1 + c_{b} \cdot (1 - \sigma^{*}) \right]$$

(B.20) re-group c_b terms of (B.19) to arrive at eqn. (8)

APPENDIX C

The intercept point of σ_d between stages 3 and 4 of Kocks-Mecking work hardening can first be evaluated and used to determine c₂ of eqn. (1). This evaluation is accomplished for each curvilinear Voce portion in the Θ versus σ_v plot, from which c_2 can then be computed, correspondingly. The intercept point of σ_d between stages 3 and 4 is evaluated by using the equality of eqn. (6). An equivalence in Θ_1 at the intercept point between stages 3 and 4 is written for Θ_3 and Θ_4 as follows.

$$\Theta_3 = \Theta_4$$

(C.1) evaluate eqn. (6) at σ_{d}

$$\Theta_{o3} - c_{b3} \cdot \sigma_{d} = \Theta_{o4} - c_{b4} \cdot \sigma_{d}$$

 $\Theta_{o3} - c_{b3} \cdot \sigma_d = \Theta_{o4} - c_{b4} \cdot \sigma_d \qquad \qquad (C.2) \text{ enter stage 3 and 4 terms for } \Theta_{oi} \text{ and } c_{bi}$

$$\Theta_{o3} - \Theta_{o4} = (c_{b3} - c_{b4}) \cdot \sigma_d$$
 (C.3) group terms of (C.2)

$$\sigma_{_{\! d}} \equiv (c_{_{\! b3}} - c_{_{\! b4}})/(\Theta_{_{\! o3}} - \Theta_{_{\! o4}})$$
 (C.4) solve for $\sigma_{_{\! d}}$

 σ_{d} , to then solve for the c_{2} value in the Voce expression within each stage of work hardening as

$$c_2 = [1 - (\sigma_d/c_1)] \cdot e^{c_3 \cdot \varepsilon}$$

(C.5) solving eqn. (1) for c_2 where σ_v equals σ_d

The values of c₁ and c₃ are needed to evaluate eqn. (C.5) for c₂. Recall that for each stage of work hardening, the vertical intercept of eqn. (5) at zero stress is the constant Θ_0 (that equals $c_3 \cdot c_1$ from eqn. 4g) and the linear slope c_b (which equals c₃ from eqn. 4g) is the softening factor coefficient.

DISTRIBUTION

Email—Internal

Name	Org.	Sandia Email Address
Joshua Yee	08262	jkyee@sandia.gov
Technical Library	1911	sanddocs@sandia.gov

Email—External

Name	Company Email Address	Company Name

Hardcopy—Internal

Number of Copies	Name	Org.	Mailstop

Hardcopy—External

Number of Copies	Name	Company Name and Company Mailing Address

This page left blank



Sandia National Laboratories is a multimission laboratory managed and operated by National Technology & Engineering Solutions of Sandia LLC, a wholly owned subsidiary of Honeywell International Inc. for the U.S. Department of Energy's National Nuclear Security Administration under contract DE-NA0003525.